Carbohydrate Polymers 151 (2016) 480–487

Contents lists available at ScienceDirect

Carbohydrate Polymers

journal homepage: www.elsevier.com/locate/carbpol

^{13}C NMR assignments of regenerated cellulose from solid-state 2D NMR spectroscopy

Alexander Idström[a], Staffan Schantz[b], Johan Sundberg[a,c], Bradley F. Chmelka[d], Paul Gatenholm[a,c], Lars Nordstierna[a,*]

[a] Department of Chemistry and Chemical Engineering, Chalmers University of Technology, SE-41296 Göteborg, Sweden
[b] AstraZeneca R&D, SE-43150 Mölndal, Sweden
[c] Wallenberg Wood Science Center, Chalmers University of Technology, SE-41296 Göteborg, Sweden
[d] Department of Chemical Engineering, University of California, 93106 Santa Barbara, CA, United States

ARTICLE INFO

Article history:
Received 5 February 2016
Received in revised form 27 May 2016
Accepted 29 May 2016
Available online 31 May 2016

Keywords:
^{13}C CP/MAS NMR
2D correlation NMR
Regenerated cellulose
Mercerized cellulose
Assignment
Deconvolution

ABSTRACT

From the assignment of the solid-state ^{13}C NMR signals in the C4 region, distinct types of crystalline cellulose, cellulose at crystalline surfaces, and disordered cellulose can be identified and quantified. For regenerated cellulose, complete ^{13}C assignments of the other carbon regions have not previously been attainable, due to signal overlap. In this study, two-dimensional (2D) NMR correlation methods were used to resolve and assign ^{13}C signals for all carbon atoms in regenerated cellulose. ^{13}C-enriched bacterial nanocellulose was biosynthesized, dissolved, and coagulated as highly crystalline cellulose II. Specifically, four distinct ^{13}C signals were observed corresponding to conformationally different anhydroglucose units: two signals assigned to crystalline moieties and two signals assigned to non-crystalline species. The C1, C4 and C6 regions for cellulose II were fully examined by global spectral deconvolution, which yielded qualitative trends of the relative populations of the different cellulose moieties, as a function of wetting and drying treatments.

1. Introduction

It is well-known that the cellulose structure possesses complexity at a range of different length scales (Klemm, Heublein, Fink, & Bohn, 2005). Cellulose is a polysaccharide and consists of linearly linked β-D-glucose residues (anhydroglucose units, AGUs), but the length and supramolecular structure of the cellulose chains vary depending on origin and treatment. As for most polymers, cellulose can be crystalline, semicrystalline or amorphous. Native cellulose consists of two different crystalline forms, cellulose Iα and Iβ (Atalla & VanderHart, 1999; VanderHart & Atalla, 1984). Another allomorph, cellulose II (Zugenmaier, 2008), is generated irreversibly from native cellulose by mercerization (swelling) (Kolpak & Blackwell, 1978; Kolpak, Weih, & Blackwell, 1978) or by regeneration (dissolution and coagulation) (O'Sullivan, 1997).

The conversion from native to regenerated cellulose has recently gained a great deal of scientific attention. Textile fibers produced from wood pulp could be an alternative to traditionally used cotton based fibers (Dawson, 2012). In addition to fibers, regenerated cellulose can also be formed as films, foams, or pellets (Isik, Sardon, & Mecerreyes, 2014; Pang et al., 2014; Zhang, Li, & Yu, 2010). Dissolution of cellulose also permits chemical modification using traditional solution chemistries (Feng & Chen, 2008).

To fully utilize such materials, a thorough understanding of the supramolecular structure of regenerated cellulose is important. For native cellulose, solid-state nuclear magnetic resonance (NMR) spectroscopy studies (Foston, 2014; Larsson, Wickholm, & Iversen, 1997; Newman & Hemmingson, 1995; Wickholm, Larsson, & Iversen, 1998) have, together with other methods, such as XRD (Ahvenainen, Kontro, & Svedström, 2016; Terinte, Ibbett, & Schuster, 2011), been able to clarify the constitution of the elementary fibrils and the fibril aggregates in cellulose fibers. These findings have been key to increasing the value of native cellulose products (O'Sullivan, 1997). The corresponding structure of regenerated cellulose, however, has not been investigated to the same extent and the supramolecular structure is therefore not fully known.

* Corresponding author.
E-mail addresses: idstrom@chalmers.se (A. Idström), staffan.schantz@astrazeneca.com (S. Schantz), johan.sundberg@chalmers.se (J. Sundberg), bradc@engineering.ucsb.edu (B.F. Chmelka), paul.gatenholm@chalmers.se (P. Gatenholm), lars.nordstierna@chalmers.se (L. Nordstierna).

http://dx.doi.org/10.1016/j.carbpol.2016.05.107
0144-8617/

From solid-state 1D ^{13}C CP/MAS NMR, information about the local chemical composition and structure of the cellulose material can be acquired. Regardless of cellulose allomorph, the signals from the different carbon atoms in the AGUs appear at certain isotropic ^{13}C chemical shifts in the NMR spectrum (Gast, Atalla, & McKelvey, 1980). For example, these include ^{13}C signals from C1 moieties (104–108 ppm), C4 moieties (82–90 ppm), a cluster of signals from C2, C3 and C5 carbon atoms (70–78 ppm), and finally C6 moieties (60–68 ppm) (Gast et al., 1980). Different allomorphs, e.g., cellulose I or cellulose II, each yield a resolved ^{13}C NMR spectrum, with characteristic signals with positions and intensities that make it possible to distinguish between the different forms.

The C4 region shows relatively well resolved signals, compared to the other ^{13}C regions, and for both native and regenerated cellulose spectral deconvolution enables the C4 ^{13}C signals to be assigned in different fibril environments. For regenerated cellulose, two signals, at 88.9 and 87.7 ppm, have been attributed to be from crystalline cellulose II (Ibbett, Domvoglou, & Fasching, 2007; Newman & Davidson, 2004), as depicted in Fig. 1. A narrow signal at 86.2 ppm has been assigned to the crystalline surface species and a broad one at 83.8 ppm to cellulose in disordered regions (Ibbett et al., 2007). The narrow signal at 84.8 ppm has also, tentatively, been assigned to cellulose at crystalline surfaces (Zuckerstätter, Terinte, Sixta, & Schuster, 2013). From the C4 ^{13}C signals, square cross-sectional cellulose models of elementary fibrils and fibril aggregates have been proposed for native (Larsson et al., 1997; Wickholm et al., 1998), and for regenerated cellulose (Zuckerstätter et al., 2013), respectively. Using these models, dimensions of elementary fibrils and fibril aggregates (Gårdebjer et al., 2015; Newman, 1999; Wickholm et al., 1998), crystallinity index (CI) (Lee et al., 2016; Park, Johnson, Ishizawa, Parilla, & Davis, 2009) as well as specific surface area (Chunilall, Bush, Larsson, Iversen, & Kindness, 2010) have been estimated and structural changes of the material, for example upon drying and rewetting, have been monitored (Idström, Brelid, Nydén, & Nordstierna, 2013; Östlund, Idström, Olsson, Larsson, & Nordstierna, 2013).

Equivalent features, with ^{13}C signals originating from different parts of the fibril model should also be observed for the other ^{13}C atoms in the AGU, though these have been more difficult to assign due to signal overlap. From multidimensional NMR methods, correlated signal intensity between directly bonded ^{13}C atoms can be distinguished. With these methods, it is possible to follow the magnetization transfer from a given C4 atom to other ^{13}C atoms to which it is covalently bonded in the AGU.

In ^{13}C solid-state NMR spectroscopy, the natural abundance of ^{13}C (~1%) provides sufficiently high signal-to-noise to acquire 1D spectrum of cellulose. In corresponding homonuclear 2D NMR spectroscopy, the signal intensity is however far too weak due to the low concentration of ^{13}C–^{13}C spin correlations. Using ^{13}C-enriched material, Kono et al. have assigned, by multidimensional NMR, the isotropic ^{13}C chemical shifts for all AGU carbons in two different crystalline molecular conformations of mercerized cellulose II (Kono & Numata, 2004; Kono, Numata, Erata, & Takai, 2004). Cadars et al. investigated correlations in solid disordered materials, for example in cellulose (Cadars, Lesage, & Emsley, 2005). There are however still unassigned signals, for all carbon regions in both mercerized and regenerated cellulose, indicating the presence of additional but not confirmed AGU residues.

In this study, ^{13}C-enriched bacterial nanocellulose (BNC) was dissolved in an ionic liquid and coagulated in water as beads to obtain regenerated cellulose with a high degree of cellulose II crystallinity. A complete spectral assignment of regenerated cellulose II, including the isotropic ^{13}C chemical shifts of carbon atoms in four distinguishable AGU conformations, was performed with the use of 2D $^{13}C\{^{13}C\}$ NMR correlation spectroscopy. The complete assignment made it possible to suggest a global spectral deconvolution of the specific C1, C4, and C6 regions for regenerated cellulose. A corresponding study was also carried out for cellulose mercerized in alkali solution.

2. Materials and methods

2.1. Production of ^{13}C-enriched bacterial nanocellulose

Bacterial nanocellulose enriched with 10% ^{13}C was produced using a modified Hestrin Schramm (HS) medium (Hestrin & Schramm, 1954) (9 g D-glucose monohydrate, 1 g D-glucose-$^{13}C_6$, 5 g peptone from soymeal, 2.5 g yeast extract, 2.7 g Na_2HPO_4, 1.15 g citric acid monohydrate, in 0.5 l Milli-Q water). The pH was set to 5.0 using 2 M HCl. All chemicals were purchased from Sigma Aldrich and used as received. The medium was sterilized by filtration through a 0.1 μm filter into a sterile bottle, inoculated with Gluconacetobacter xylinus subspecies sucrofermentas BRP2001 (700178^{TM}, LGC Promochem AB, Borås Sweden) and incubated overnight at 30 °C. The inoculated medium was transferred to 12-well plates, 3 ml per well, and the plates were incubated at 30 °C for 96 h. After culture completion the BNC was purified from bacteria by immersion in 0.1 M NaOH overnight at room temperature. The BNC was transferred to bulk amounts of fresh NaOH every 2 h until clean and subsequently washed thoroughly in Milli-Q water until the pH was neutralized. The clean BNC was autoclaved wet at 121 °C for 20 min (Varioklav 135T) to avoid further microbial action until usage.

2.2. Production of ^{13}C-enriched regenerated cellulose

The regenerated material was produced as described previously (Östlund et al., 2013). The ^{13}C-enriched BNC was freeze-dried using a Scanvac Coolsafe 110 freeze dryer. 1-Ethyl-3-methylimidazolium acetate, EMIMAc, (LOT STBC9122 V) was purchased from Sigma Aldrich and used as received. 2 wt% of dry cellulose was dissolved in EMIMAc at 50 °C for 5 h. The solution was added drop-wise to Milli-Q water at room temperature in order to coagulate. The choice of water as coagulation medium was to obtain a material with as high crystallinity as possible (Östlund et al., 2013). The produced material was subsequently rinsed several times in Milli-Q water and analyzed by solid-state NMR spectroscopy.

2.3. Production of ^{13}C-enriched mercerized cellulose

The mercerized material was produced according to the procedure by Kono et al. (Kono et al., 2004). NaOH was purchased from Sigma Aldrich and was used as received. The ^{13}C-enriched BNC was added to an aqueous NaOH solution up to a final concentration of 3 wt% BNC and 20 wt% NaOH. The mixture was left under continuous stirring in ambient temperature for 2 weeks. The resulting material was subsequently washed in Milli-Q water, and centrifuged several times to remove residual NaOH, and analyzed with solid-state NMR spectroscopy.

2.4. Production of regenerated cellulose with natural abundance ^{13}C

Regenerated cellulose with natural abundance ^{13}C was produced for drying and wetting studies. Bleached Kraft Eucalyptus dissolving pulp was provided by Bahia Pulp S.A., Brazil. 2 wt% of the pulp was dissolved in EMIMAc and coagulated in water, as described above. The regenerated samples were dispersed in Milli-Q water and then dried in oven at 105 °C for 3 h. This was repeated

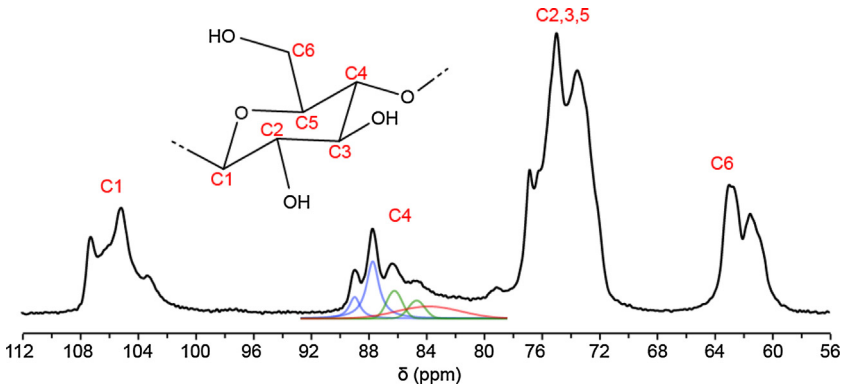

Fig. 1. 1D ^{13}C CP/MAS NMR spectrum of regenerated cellulose. The anhydroglucose unit (AGU) is shown as an inset. Deconvolution of the C4 region of the spectrum, according to Zuckerstätter et al. (2013) is also shown, with fit signals that are attributed to crystalline cellulose II shown in blue, signals from crystalline surfaces in green and signals from disordered material in red. (For interpretation of the references to colour in this figure legend, the reader is referred to the web version of this article.)

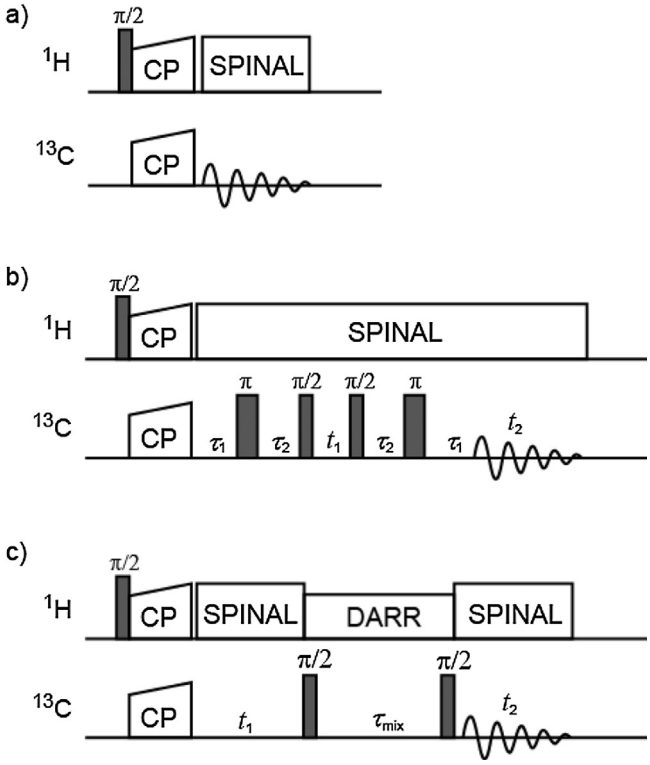

Fig. 2. NMR pulse sequences for (a) 1D ^{13}C{^{1}H} CP/MAS, (b)2D ^{13}C{^{13}C} refocused INADEQUATE, and (c) 2D ^{13}C{^{13}C} PDSD with DARR experiments.

up to 7 times and after each drying a fraction of the sample was removed for solid-state NMR analysis.

2.5. Solid-state NMR spectroscopy

All NMR experiments were performed on a Varian Inova-600 operating at 14.7 T and equipped with a 3.2 mm solid-state magic-angle-spinning (MAS) probe head. Measurements were conducted at 298 K with a MAS spinning rate of 15 kHz. Three different NMR-pulse sequences, shown in Fig. 2, were used in this project: the 1D experiment Cross-Polarization Magic-Angle Spinning (CP/MAS) and two 2D experiments denoted refocused INADEQUATE (Incredible Natural Abundance DoublE QUAntum Transfer Experiment) and PDSD (Proton Driven Spin Diffusion) with DARR (Diffusion Assisted Rotational Recoupling). The ^{1}H decoupling sequence SPINAL-64 was used in all of the NMR experiments. The ^{13}C chemical shifts reported for the cellulose carbons vary in scientific reports, due to the use of different reference substances. In the present article, isotropic ^{13}C chemical shifts were referenced to adamantane as external standard (Morcombe & Zilm, 2003), according to IUPAC recommendations (Harris et al., 2008).

One-dimensional (1D) ^{13}C Cross-Polarization Magic-Angle Spinning (CP/MAS) spectra were acquired using the pulse sequence shown in Fig. 2a with a 2.9 μs ^{1}H 90° pulse, 1200 μs CP-contact time, 35 ms acquisition time with proton decoupling, and 4 s recycle delay. The number of acquisitions for the 1D ^{13}C{^{1}H} NMR spectra was 800 for the ^{13}C-enriched samples and 16384 for those with ^{13}C in natural abundance. The CP/MAS pulse sequence is not inherently quantitative, and the obtained integrals can differ depending on if the studied material is crystalline or amorphous. However, for the studied cellulose material, choosing a short CP-contact time (below 1500 μs) quantitative measurements could be conducted (Larsson et al., 1997).

Two-dimensional (2D) ^{13}C{^{13}C} refocused INADEQUATE spectra (pulse sequence shown in Fig. 2b) were acquired to detect covalently bonded *J*-coupled ^{13}C–^{13}C spin pairs. In this experiment, directly bonded carbon atoms yield correlated ^{13}C signals in the single-quantum (SQ) and double-quantum (DQ) dimensions, the latter at the sum of their frequencies. For samples with high ^{13}C abundances, correlated signals could also be observed involving a third carbon atom (visible as a negative signal at the chemical shift of the third), at the combined frequency of the first two in the DQ-dimension (Cadars et al., 2007; Ernst, Bodenhausen, & Wokaun, 1987). Acquisition parameters included 2.9 and 4.0 μs, ^{1}H and ^{13}C 90° pulses, respectively, a 700 μs CP-contact time, 15 ms acquisition time, 3 ms refocusing delay (τ_1 and τ_2), 2 s recycle delay, and 128 points in the direct dimension, and 512 points in the indirect dimension. The pulse sequence was optimized by using uniformly ^{13}C-enriched glucose.

2D ^{13}C{^{13}C} dipolar-mediated NMR spectra were acquired with Proton-Driven Spin Diffusion (PDSD) and Diffusion-Assisted Rotational Recoupling (DARR) (pulse sequence shown in Fig. 2c) to measure and correlate the isotropic ^{13}C chemical shifts of dipole-dipole-coupled ^{13}C–^{13}C spin pairs in different AGUs. PDSD is frequently used for studies of protein structure (Böckmann, 2006; Manolikas, Herrmann, & Meier, 2008) and is especially convenient to use for ^{13}C–^{13}C correlations, where MAS removes dipolar couplings between the ^{13}C spins. The addition of DARR, a weak RF-pulse during the mixing time (τ_{mix}), further increases the recoupling of the dipolar interactions. Cross peaks from a PDSD experiment indicate correlations between different ^{13}C nuclei through space. For the PDSD measurements 2.9 and 4.0 μs, ^{1}H and ^{13}C 90° pulse angles, respectively, were used, with 700 μs CP-contact time, 15 ms acqui-

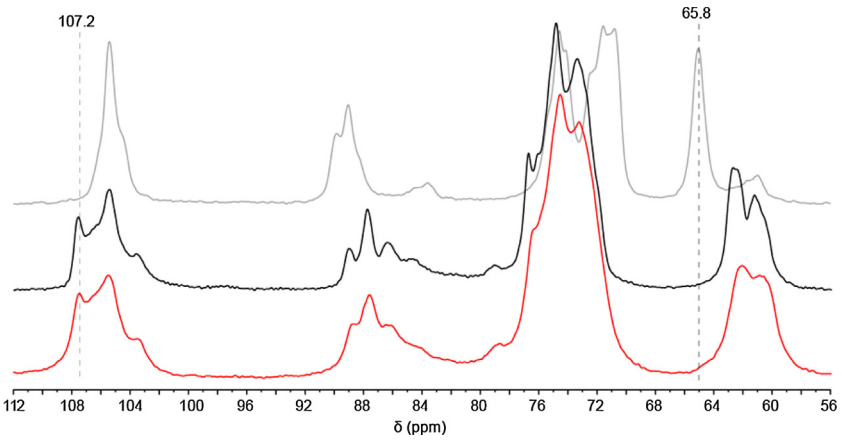

Fig. 3. 1D ^{13}C CP/MAS NMR spectra of (from top) ^{13}C-enriched BNC (grey), after regeneration (black) and after mercerization (red). (For interpretation of the references to colour in this figure legend, the reader is referred to the web version of this article.)

sition, 2 s recycle delay, 128 points in the direct dimension, and 1024 points in the indirect dimension.

2.6. X-ray diffraction

X-ray diffraction (XRD) measurements were recorded on a Siemens D5000 diffractometer using CuKα radiation (λ = 1.5418 Å). The diffractograms were obtained using a scintillation detector and a Bragg-Brentano geometry. The X-ray source was operated at 45 kV and 40 mA. Scans were obtained from 10 to 40° 2θ in 0.05° steps for 10 s per step.

3. Results and discussion

The ^{13}C-enriched BNC was dissolved in EMIMAc and coagulated in water using the method described above and the ^{13}C CP/MAS NMR spectrum of the material is shown (center/black) in Fig. 3. Conversion to crystalline cellulose II is evidenced by the appearance of a characteristic cellulose II signal at 107.2 ppm (Zuckerstätter et al., 2009). In addition, based on the absence of the characteristic cellulose I signal at 65.8 ppm, no signs of the starting material (top/grey) could be detected in the regenerated material. A CI of 79% of cellulose II was obtained for the regenerated material using XRD peak-height method (Park, Baker, Himmel, Parilla, & Johnson, 2010; Segal, Creely, Martin, & Conrad, 1959), which is in line with previous work (Olsson, Idström, Nordstierna, & Westman, 2014). The ^{13}C CP/MAS NMR spectrum of the mercerized ^{13}C-enriched BNC is shown in Fig. 3 (bottom/red). It should be noted that the obtained CI should not be considered as absolute since results could differ substantially depending on analysis method used (Park et al., 2010).

3.1. Spectral assignment

In the C4 region of the ^{13}C CP/MAS NMR spectrum of regenerated cellulose shown in Fig. 1, two ^{13}C signals from crystalline cellulose II (shown in blue) are present. These have previously been assigned to two distinct AGU conformations, referred to as residue A and residue B by Kono et al. (Kono et al., 2004). In this report, the ^{13}C atoms in residue A are distinguished from those in residue B by the addition of a prime symbol (′) for those in residue B. The ^{13}C signal with the smallest chemical shift (87.7 ppm) of the two signals was assigned as C4, belonging to residue A, and that corresponding to the largest shift (88.9 ppm) was assigned as C4′, belonging to residue B. In the previous assignment presented by Kono et al. (Kono et al., 2004), hydrolysis of the mercerized cellulose had been performed, and only strong crystalline correlations are presented in their publication. In the present study, the hydrolysis step was omitted, and it was therefore possible to distinguish two additional AGU conformations. Conformation three is designated here as residue C, marked with a star symbol (*), while conformation four corresponds to residue D, marked by two stars (**). The C4 signal of residue C was previously assigned by Zuckerstätter et al. as a crystalline surface signal at the shift 86.2 ppm shift (Zuckerstätter et al., 2013). Similarly, the C4 signal of residue D was previously tentatively assigned as a crystalline surface signal at the shift 84.8 ppm by the same authors. Complete assignments of residue C and D for all AGU carbons have not previously been reported in the literature to the best of our knowledge.

Table 1
Isotropic ^{13}C chemical shift assignments (in ppm) for cellulose II.[a]

	C1	C2	C3	C4	C5	C6
Residue A	107.2	72.9	73.5	87.7	75.0	62.5
Residue B	105.1	74.8	76.8	88.9	72.0	63.2
Residue C	106.4	72.8	73.4	86.2	75.9	61.7
Residue D	103.3	73.7	74.5	84.8	74.5	61.3

[a] The chemical shift values are estimated to be accurate to ±0.1 ppm.

The complete assignments of the ^{13}C NMR signals associated with the distinct carbon moieties in cellulose II, obtained using solid-state 2D ^{13}C{^{13}C} refocused INADEQUATE and PDSD with DARR, are summarized in Table 1. Solid-state ^{13}C NMR spectra for the ^{13}C-enriched BNC, regenerated cellulose, and mercerized cellulose, respectively, as well as a detailed description of the assignment method used for all four residues of the regenerated cellulose can be found in the Supplementary material.

One should note that we here present assignments of C3 and C5 for residue A (at 73.5 and 75.0 ppm, respectively) that differ from those reported by Kono et al. (at 75.2 and 74.4 ppm, respectively) for mercerized cellulose II (Kono & Numata, 2004; Kono et al., 2004). Experimental results that advocated the new assignment include strong correlated intensity at 73.5 ppm in the single-quantum dimension and at 161.2 ppm in the double-quantum dimension of the 2D ^{13}C{^{13}C} refocused INADEQUATE spectrum (Fig. 4, inset), which are consistent with the new assignments of these signals to *J* coupled C3 and C4 (87.7 ppm). An intensity correlation is also visible at 72.9 ppm (C2) and at 146.5 ppm (C3). A corresponding correlation is also present in the PDSD with DARR spectrum as a very strong cross peak between 87.7 ppm and 73.5 ppm (Fig. 5, inset). In addition, the ^{13}C signal at 75.0 ppm, newly assigned, to carbon atom C5 is correlated with the signal at 62.5 ppm from the C6 (DQ-frequency 137.4 ppm). To verify that this assignment was not associated with a difference in crystalline structure between

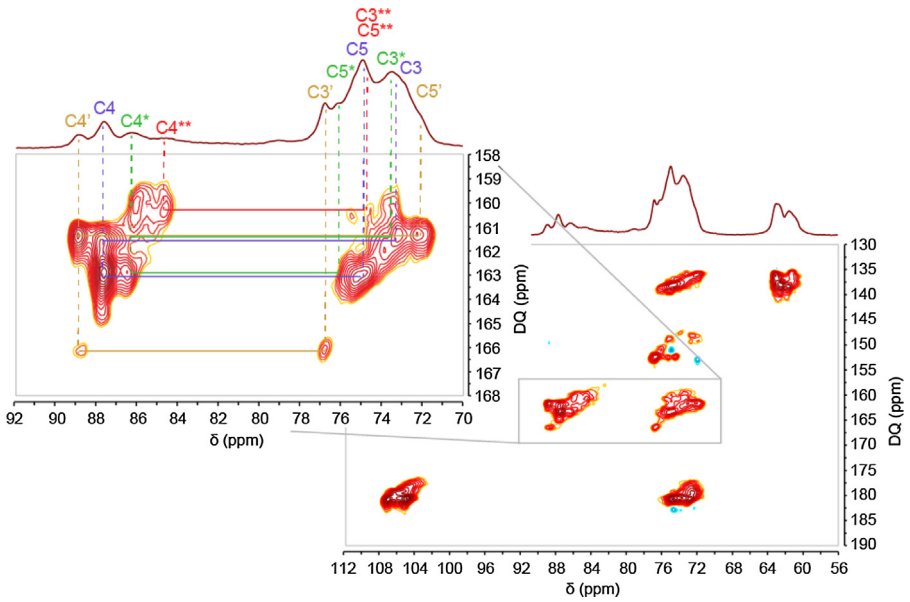

Fig. 4. Solid-state 2D $^{13}C\{^{13}C\}$ refocused INADEQUATE (J-mediated) NMR spectrum of ^{13}C-enriched regenerated cellulose. Inset shows C3-C4-C5 intensity correlations of residue A (blue), residue B (orange), residue C (green), and residue D (red). (For interpretation of the references to colour in this figure legend, the reader is referred to the web version of this article.)

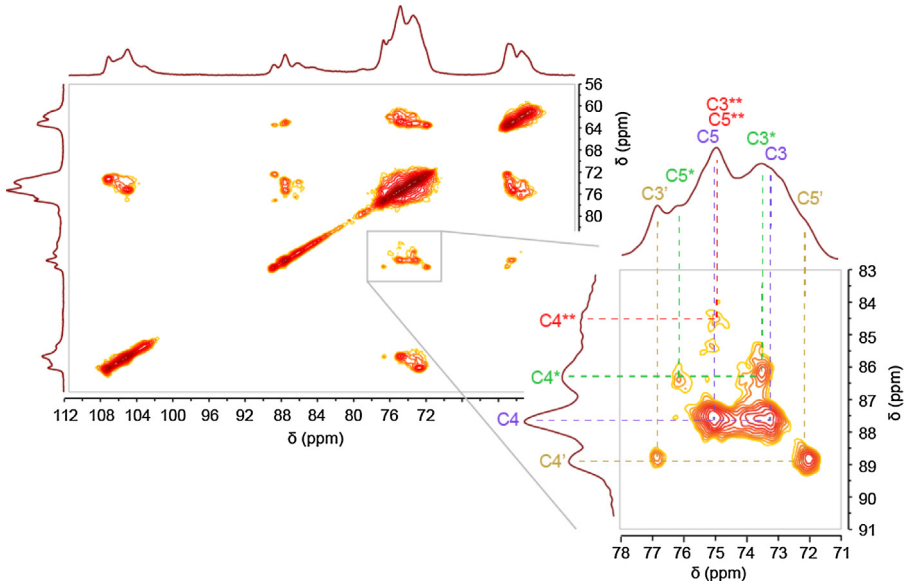

Fig. 5. Solid-state 2D $^{13}C\{^{13}C\}$ dipolar-mediated NMR spectrum acquired with PDSD with DARR of ^{13}C-enriched regenerated cellulose. Inset shows correlated signals between residue A (blue), residue B (orange), residue C (green), and residue D (red). (For interpretation of the references to colour in this figure legend, the reader is referred to the web version of this article.)

regenerated and mercerized cellulose, ^{13}C-enriched mercerized cellulose was produced and studied using the same NMR correlation methods as for regenerated cellulose. Results from the 2D $^{13}C\{^{13}C\}$ refocused INADEQUATE (through-bond *J*-mediated) and PDSD-DARR experiments (through-space dipolar-mediated) generated identical spectral assignments for both regenerated and mercerized cellulose (see Supplementary material). It was therefore concluded that regenerated and mercerized cellulose have the same crystalline structure and that the proposed new assignment for C3 and C5 of residue A is valid for both these materials.

For regenerated cellulose, the 2D $^{13}C\{^{13}C\}$ dipolar-mediated PDSD-DARR spectrum in Fig. 5 shows a weak intensity correlation between the ^{13}C signals associated with carbon atoms C1 and C4, as well as between carbon atoms C1′ and C4′. It is noteworthy that no correlated signal intensities were detected for ^{13}C signals associated with the carbon-atom pairs C1-C4′ or C1′-C4. This supported the two-chain structure of cellulose II proposed by Kono et al. (Kono et al., 2004), who reported intensity correlations between C1 and C4 nuclei within one type of residue, though not between C1 and C4 nuclei of different types of residues. Kono et al. concluded that crystalline cellulose II, consists of two types of AGU, with different molecular conformations, that do not belong to the same chain, i.e., the chains in cellulose II are constructed with -A-A- and -B-B- repeating units, and few if any -A-B- moieties (Kono et al., 2004). This result is also in good agreement with previous results obtained from XRD (Kolpak & Blackwell, 1976; Langan, Nishiyama, & Chanzy, 2001) and molecular dynamics simulations (Kroon-Batenburg, Bouma, & Kroon, 1996). For residue C

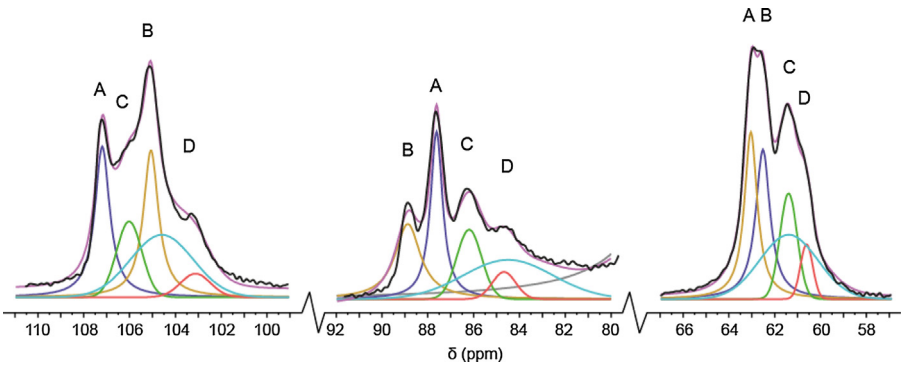

Fig. 6. The C1 (left), C4 (center), and C6 (right) regions of the 1D ^{13}C CP/MAS NMR spectrum (black) together with their spectral deconvolutions of ^{13}C-enriched regenerated cellulose: residue A (blue), residue B (orange), residue C (green), residue D (red), disordered cellulose (turquoise). A correction for the large signals from the C2, C3, and C5 region (grey) in the C4 region is also shown. The sum of the deconvolution is shown in cerise color. (For interpretation of the references to colour in this figure legend, the reader is referred to the web version of this article.)

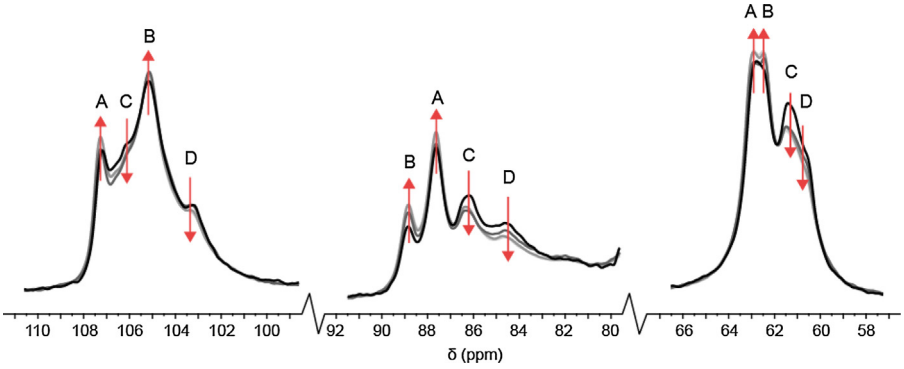

Fig. 7. The C1, C4 and C6 regions of the 1D ^{13}C CP/MAS NMR spectrum of regenerated Bahia pulp treated by drying and wetting cycles. Never-dried sample (black), sample dried in oven one time (dark grey), 3 times (grey) and 5 times (light grey) are shown. The apparent trends when applying additional drying and wetting cycles are shown with red arrows. (For interpretation of the references to colour in this figure legend, the reader is referred to the web version of this article.)

and residue D, respectively, no clear ^{13}C–^{13}C intensity correlations could be detected in the dipolar-mediated PDSD-DARR spectrum between the signals of carbon atoms C1 and C4. It is therefore not clear whether residues C and D belong to different cellulose polymer chains, i.e. -C-C- and -D-D-, or if they are within the same chain as -C-D- moieties. Additional studies have to be performed to resolve this issue.

3.2. Spectral deconvolution

Previously, only deconvolutions of the C4 region of the 1D ^{13}C NMR spectra of cellulose II have been reported in the literature (Ibbett et al., 2007; Zuckerstätter et al., 2009, 2013). While the C2, C3, and C5 signals overlap too severely to accomplish a deconvolution, the C1 and C6 regions could still be used. Using the isotropic ^{13}C chemical shift values obtained from the complete spectral assignment enabled by the improved resolution of the 2D ^{13}C{^{13}C} NMR correlation spectra, a simultaneous global deconvolution of the C1, C4 and C6 regions could be performed.

The reliability of the deconvolution included boundary conditions that were set as follows. All chemical shifts were fixed according to the new assignments in Table 1. In addition, the isotropic ^{13}C chemical shifts associated with each carbon atom of the disordered cellulose were acquired from CP/MAS experiments with short pre-pulse relaxation delays (Wickholm et al., 1998). ^{13}C signals referred to as 'crystalline', e.g., residues A and B, were assumed to have Lorentzian lineshapes. Other ^{13}C signals, such as those from residues C and D and from disordered cellulose, were assumed to have Gaussian lineshapes. The choice of lineshape follows the analysis according to Larsson et al. (Larsson & Westlund, 2005). It is noted that the use of Gaussian lineshapes on overlapping signals from disordered cellulose moieties could be suboptimal, however this is adequate for the discussion concerning arrangements of AGU residues. All AGU residues, whether crystalline or near a crystalline surface, consist of equal relative fractions of carbon atoms. It could therefore be noted that, e.g., AGU residue A should have the same relative contribution in the C1 region, e.g. 25%, as it has in the C4 and C6 regions. The same is true for each of the different AGU residues, i.e., one type of AGU residue is expected to have the same relative stoichiometric contributions in the different residues and therefore also with respect to the relative integrals of the ^{13}C signals in the different spectral regions. In addition, assuming that the previous assignment by Kono et al. is correct, for sufficiently large crystals the relative fraction of AGU residue A should be very similar, if not identical, to that of AGU residue B in a cellulose II crystal (O'Sullivan, 1997), so that their integrated signals are expected to be the same. Following these constraints on integral balances, the linewidths and the amplitudes of all ^{13}C signals were calculated by the global deconvolution using a least-squares fitting of parameters in lineshape functions with nonlinear parameter dependence by using the Levenberg-Marquardt method described in Supplementary material.

Each region (C1, C4, and C6) of the 1D ^{13}C CP/MAS spectrum of the ^{13}C-enriched regenerated cellulose in Fig. 6 was deconvoluted into five ^{13}C signals, two of which were fit with Lorentzian lineshapes and three with Gaussian lineshapes. In the C4 region, an additional Gaussian signal was added to account for the overlapping tail contribution from the C2, C3 and C5 signals. The overall deconvolutions of the C1, C4 and C6 regions are shown in Fig. 6, with spectral fitting parameters obtained for the three regions shown

Table 2
Spectral fitting parameters obtained for the C1, C4, and C6 regions.

	C1			C4			C6			
	Shift	FWHM	Amp	Shift	FWHM	Amp	Shift	FWHM	Amp	Rel area
Residue A	107.2	119	0.12	87.7	96	0.14	62.5	112	0.14	25.5%
Residue B	105.1	121	0.12	88.9	201	0.07	63.2	100	0.16	25.5%
Residue C	106.4	197	0.06	86.2	193	0.06	61.7	132	0.10	14.4%
Residue D	103.3	233	0.02	84.8	181	0.02	61.3	94	0.05	5.3%
Amorph	104.6	486	0.05	75.8	695	0.03	61.44	443	0.06	29.3%

in Table 2. It should be noted that if the ^{13}C signals associated with residue A and residue B possess independent integrals in the regression analysis, their relative difference ends up to be merely 3% which strengthen previous findings of equal amounts of A and B in the cellulose II crystal.

The isotropic ^{13}C chemical shifts and linewidths obtained from global deconvolution of the signal intensity in the C4 region of the spectrum correspond well to those reported by others (Zuckerstätter et al., 2009, 2013). There is an appearance of different linewidth for signals originating from the same AGU residue when comparing the three carbon regions. This may be due to different transverse relaxation properties, but a full analysis of spin dynamics is beyond the scope of this work.

Zuckerstätter previously assigned residue C as a surface signals and residue D tentatively as a surface signal (Zuckerstätter et al., 2013). It could be noted from Table 2 that the relative integral values obtained for residue C and D differs substantially, being 14.4% for residue C and 5.3% for residue D. It should be pointed out that there is no direct expectation on the quantitative relationship between C and D since there is so far no existing elementary fibril model of cellulose II equivalent to the well-known square cross-sectional model of cellulose I. Questions to be raised, is there a conformational change of the fibril which generates excessive C positions compared to D, or are there different exposed surfaces in cellulose II?

It has previously been shown that treating regenerated cellulose to drying and wetting cycles results in an increase of the crystallinity (Östlund et al., 2013). This can be followed in the C4 region as an increase of signal intensity from crystalline domains, and a corresponding decrease of the signal intensity originating from crystalline surfaces. With the proposed assignment and deconvolution, an increase in the ^{13}C signals from moieties in crystalline environments and a corresponding decrease in those from crystalline surface should also be seen in the C1 and C6 regions. A reference sample (with natural abundance ^{13}C) was produced from Bahia pulp, dissolved in EMIMAc and coagulated in water. The 1D ^{13}C CP/MAS NMR spectrum of the resulting material is shown in Fig. 7 (black). This material was then dispersed in Milli-Q water, dried in oven at 105 °C for 3 h, one time, 3 times and 7 times and the corresponding ^{13}C CP/MAS spectra acquired again [Fig. 7]. All spectra were normalized over the entire spectral region (Östlund et al., 2013).

With increased number of drying cycles an increase of the ^{13}C signals from crystalline domains (residue A and residue B) and a decrease of the ^{13}C signals corresponding to residue C and residue D can be seen in the C4 region. The apparent trends are indicated with red arrows. Identical trends could be seen for the C1 and C6 regions, which could indicate that residue C and D are near surfaces and suggest co-crystallization. However, due to the overlapping features of the deconvolution proposed, the reduced intensities could also be due to conversion of amorphous cellulose into the crystalline form. More work has to be performed to resolve this issue. Full spectra of all materials in the drying and wetting study are provided in the Supplementary material.

4. Conclusions

In this work, new and expanded insights about the solid-state NMR characterization of regenerated cellulose material have been reported. The solid-state 2D $^{13}C\{^{13}C\}$ NMR correlation experiments show that, in addition to disordered cellulose, four ^{13}C signals are resolved from different types of anhydroglucose units (AGUs) that are formed when cellulose material is regenerated. The enhanced resolution provided by the 2D NMR analyses enable assignments of the isotropic ^{13}C chemical shifts for all carbon atoms in the four different AGUs, along with revised assignments for carbon atoms C3 and C5 for one of the crystalline AGUs. Based on the chemical shift assignments from the 2D NMR data, a global spectral deconvolution was applied to the 1D ^{13}C CP/MAS NMR spectrum of regenerated cellulose, including the signals of the C1 and C6 regions. The resulting isotropic ^{13}C chemical shifts, linewidths, and their intensity correlations represent important metrics in the effort to correlate the molecular compositions and structures with the macroscopic properties of cellulose-based materials. Materials based on regenerated cellulose are currently of high interest for the development of a range of applications and products where fundamental molecular and nanoscale characterization is required. The comprehensive chemical shift assignment reported in this work can thus serve as a key tool in future studies of polymer matrix based nanocomposites, spun textile fibers, and other new materials based on regenerated cellulose.

Conflict of interest

The authors declare no competing financial interest.

Acknowledgments

This work has been carried out within the framework of Avancell—Centre for Fibre Engineering. Financial support from the Swedish Foundation, Södra Skogsägarnas stiftelse för forskning, utveckling och utbildning, is gratefully acknowledged. The Knut and Alice Wallenberg Foundation is gratefully acknowledged for funding the Wallenberg Wood Science Center. The NMR measurements were carried out at the Swedish NMR Centre, Göteborg, Sweden with equipment partly funded by Troëdssons forskningsfond. The work at UCSB was supported by the Institute for Collaborative Biotechnologies through grant W911NF-09-0001 from the USARO. The collaboration arose from a series of bilateral workshops between Chalmers and UCSB, with support in part from the U.S. National Science Foundation and Chalmers University of Technology.

Appendix A. Supplementary data

Supplementary data associated with this article can be found, in the online version, at http://dx.doi.org/10.1016/j.carbpol.2016.05.107.

References

Ahvenainen, P., Kontro, I., & Svedström, K. (2016). Comparison of sample crystallinity determination methods by X-ray diffraction for challenging cellulose I materials. *Cellulose*, *23*(2), 1073–1086.

Atalla, R. H., & VanderHart, D. L. (1999). The role of solid state ^{13}C NMR spectroscopy in studies of the nature of native celluloses. *Solid State Nuclear Magnetic Resonance*, *15*(1), 1–19.

Böckmann, A. (2006). Structural and dynamic studies of proteins by high-resolution solid-state NMR. *Comptes Rendus Chimie*, *9*(3–4), 381–392.

Cadars, S., Lesage, A., & Emsley, L. (2005). Chemical shift correlations in disordered solids. *Journal of the American Chemical Society*, *127*(12), 4466–4476.

Cadars, S., Sein, J., Duma, L., Lesage, A., Pham, T. N., Baltisberger, J. H., et al. (2007). The refocused INADEQUATE MAS NMR experiment in multiple spin-systems: interpreting observed correlation peaks and optimising lineshapes. *Journal of Magnetic Resonance*, *188*(1), 24–34.

Chunilall, V., Bush, T., Larsson, P.-T., Iversen, T., & Kindness, A. (2010). A CP/MAS ^{13}C NMR study of cellulose fibril aggregation in eucalyptus dissolving pulps during drying and the correlation between aggregate dimensions and chemical reactivity. *Holzforschung*, *64*(6), 683.

Dawson, T. (2012). Progress towards a greener textile industry. *Coloration Technology*, *128*(1), 1–8.

Ernst, R. R., Bodenhausen, G., & Wokaun, A. (1987). *Principles of nuclear magnetic resonance in one and two dimensions*. New York: Oxford Science Publications.

Feng, L., & Chen, Z.-. (2008). Research progress on dissolution and functional modification of cellulose in ionic liquids. *Journal of Molecular Liquids*, *142*(1–3), 1–5.

Foston, M. (2014). Advances in solid-state NMR of cellulose. *Current Opinion in Biotechnology*, *27*(0), 176–184.

Gårdebjer, S., Bergstrand, A., Idström, A., Börstell, C., Naana, S., Nordstierna, L., et al. (2015). Solid-state NMR to quantify surface coverage and chain length of lactic acid modified cellulose nanocrystals, used as fillers in biodegradable composites. *Composites Science and Technology*, *107*, 1–9.

Gast, J. C., Atalla, R. H., & McKelvey, R. D. (1980). The ^{13}C N.M.R. spectra of the xylo- and cello-oligosaccharides. *Carbohydrate Research*, *84*(1), 137–146.

Harris, R. K., Becker, E. D., d Menezes, S. M. C., Granger, P., Hoffman, R. E., & Zilm, K. W. (2008). Further conventions for NMR shielding and chemical shifts: (IUPAC recommendations 2008). *Pure and Applied Chemistry*, *80*(1), 59–84.

Hestrin, S., & Schramm, M. (1954). Synthesis of cellulose by Acetobacter xylinum. II. Preparation of freeze-dried cells capable of polymerizing glucose to cellulose. *Biochemical Journal*, *58*(2), 345–352.

Ibbett, R. N., Domvoglou, D., & Fasching, M. (2007). Characterisation of the supramolecular structure of chemically and physically modified regenerated cellulosic fibres by means of high-resolution Carbon-13 solid-state NMR. *Polymer*, *48*(5), 1287–1296.

Idström, A., Brelid, H., Nydén, M., & Nordstierna, L. (2013). CP/MAS 13C NMR study of pulp hornification using nanocrystalline cellulose as a model system. *Carbohydrate Polymers*, *92*(1), 881–884.

Isik, M., Sardon, H., & Mecerreyes, D. (2014). Ionic liquids and cellulose: dissolution, chemical modification and preparation of new cellulosic materials. *International Journal of Molecular Sciences*, *15*(7), 11922.

Klemm, D., Heublein, B., Fink, H. P., & Bohn, A. (2005). Cellulose: fascinating biopolymer and sustainable raw material. *Angewandte Chemie-International Edition*, *44*(22), 3358–3393.

Kolpak, F. J., & Blackwell, J. (1976). Determination of the structure of cellulose II. *Macromolecules*, *9*(2), 273–278.

Kolpak, F. J., & Blackwell, J. (1978). Mercerization of cellulose: 2. The morphology of Mercerized cotton cellulose. *Polymer*, *19*(2), 132–135.

Kolpak, F. J., Weih, M., & Blackwell, J. (1978). Mercerization of cellulose: 1. Determination of the structure of mercerized cotton. *Polymer*, *19*(2), 123–131.

Kono, H., & Numata, Y. (2004). Two-dimensional spin-exchange solid-state NMR study of the crystal structure of cellulose II. *Polymer*, *45*(13), 4541–4547.

Kono, H., Numata, Y., Erata, T., & Takai, M. (2004). ^{13}C and ^{1}H resonance assignment of mercerized cellulose II by two-dimensional MAS NMR spectroscopies. *Macromolecules*, *37*(14), 5310–5316.

Kroon-Batenburg, L. M. J., Bouma, B., & Kroon, J. (1996). Stability of cellulose structures studied by MD simulations. Could mercerized cellulose II be parallel? *Macromolecules*, *29*(17), 5695–5699.

Langan, P., Nishiyama, Y., & Chanzy, H. (2001). X-ray structure of mercerized cellulose II at 1 Å resolution. *Biomacromolecules*, *2*(2), 410–416.

Larsson, P. T., & Westlund, P.-O. (2005). Line shapes in CP/MAS ^{13}C NMR spectra of cellulose I. *Spectrochimica Acta Part A: Molecular and Biomolecular Spectroscopy*, *62*(1–3), 539–546.

Larsson, P. T., Wickholm, K., & Iversen, T. (1997). A CP/MAS ^{13}C NMR investigation of molecular ordering in celluloses. *Carbohydrate Research*, *302*(1–2), 19–25.

Lee, C., Dazen, K., Kafle, K., Moore, A., Johnson, D. K., Park, S., et al. (2016). Correlations of apparent cellulose crystallinity determined by XRD, NMR, IR, raman, and SFG methods. In J. O. Rojas (Ed.), *Cellulose chemistry and properties: fibers, nanocelluloses and advanced materials* (pp. 115–131). Cham: Springer International Publishing.

Manolikas, T., Herrmann, T., & Meier, B. H. (2008). Protein structure determination from ^{13}C spin-diffusion solid-state NMR spectroscopy. *Journal of the American Chemical Society*, *130*(12), 3959–3966.

Morcombe, C. R., & Zilm, K. W. (2003). Chemical shift referencing in MAS solid state NMR. *Journal of Magnetic Resonance*, *162*(2), 479–486.

Newman, R. H., & Davidson, T. C. (2004). Molecular conformations at the cellulose-water interface. *Cellulose*, *11*(1), 23–32.

Newman, R. H., & Hemmingson, J. A. (1995). Carbon-13 NMR distinction between categories of molecular order and disorder in cellulose. *Cellulose*, *2*(2), 95–110.

Newman, R. H. (1999). Estimation of the lateral dimensions of cellulose crystallites using 13C NMR signal strengths. *Solid State Nuclear Magnetic Resonance*, *15*(1), 21–29.

O'Sullivan, A. C. (1997). Cellulose: the structure slowly unravels. *Cellulose*, *4*(3), 173–207.

Olsson, C., Idström, A., Nordstierna, L., & Westman, G. (2014). Influence of water on swelling and dissolution of cellulose in 1-ethyl-3-methylimidazolium acetate. *Carbohydrate Polymers*, *99*, 438–446.

Östlund, Å, Idström, A., Olsson, C., Larsson, P., & Nordstierna, L. (2013). Modification of crystallinity and pore size distribution in coagulated cellulose films. *Cellulose*, *20*(4), 1657–1667.

Pang, J.-H., Liu, X., Wu, M., Wu, Y.-Y., Zhang, X.-M., & Sun, R.-C. (2014). Fabrication and characterization of regenerated cellulose films using different ionic liquids. *Journal of Spectroscopy*, *2014*, 8.

Park, S., Johnson, D., Ishizawa, C., Parilla, P., & Davis, M. (2009). Measuring the crystallinity index of cellulose by solid state ^{13}C nuclear magnetic resonance. *Cellulose*, *16*(4), 641–647.

Park, S., Baker, J., Himmel, M., Parilla, P., & Johnson, D. (2010). Cellulose crystallinity index: measurement techniques and their impact on interpreting cellulase performance. *Biotechnology for Biofuels*, *3*(1), 10.

Segal, L., Creely, J. J., Martin, A. E., & Conrad, C. M. (1959). An empirical method for estimating the degree of crystallinity of native cellulose using the X-ray diffractometer. *Textile Research Journal*, *29*(10), 786–794.

Terinte, N., Ibbett, R., & Schuster, K. C. (2011). Overview on native cellulose and microcrystalline cellulose I structure studied by X-ray diffraction (WAXD): comparison between measurement techniques. *Lenzinger Berichte*, *89*, 118–131.

VanderHart, D. L., & Atalla, R. H. (1984). Studies of microstructure in native celluloses using solid-state ^{13}C NMR. *Macromolecules*, *17*(8), 1465–1472.

Wickholm, K., Larsson, P. T., & Iversen, T. (1998). Assignment of non-crystalline forms in cellulose I by CP/MAS ^{13}C NMR spectroscopy. *Carbohydrate Research*, *312*(3), 123–129.

Zhang, S., Li, F.-X., & Yu, J.-Y. (2010). Structure and properties of novel cellulose fibres produced from NaOH/PEG-treated cotton linters. *Iranian Polymer Journal*, *19*(12), 949–957.

Zuckerstätter, G., Schild, G., Wollboldt, P., Roeder, T., Weber, H. K., & Sixta, H. (2009). The elucidation of cellulose supramolecular structure by ^{13}C CP-MAS NMR. *Lenzinger Ber.*, *87*, 38–46.

Zuckerstätter, G., Terinte, N., Sixta, H., & Schuster, K. C. (2013). Novel insight into cellulose supramolecular structure through ^{13}C CP-MAS NMR spectroscopy and paramagnetic relaxation enhancement. *Carbohydrate Polymers*, *93*(1), 122–128.

Zugenmaier, P. (2008). *Crystalline cellulose and derivatives: characterization and structures*. Springer.